Ferromagnetic relaxation in 3d metals at far infrared frequencies in high magnetic fields

1990 J. Phys.: Condens. Matter 2 7187

(http://iopscience.iop.org/0953-8984/2/34/012)

J. Phys.: Condens. Matter **2** (1990) 7187–7193. Printed in the UK

Ferromagnetic relaxation in 3d metals at far infrared frequencies in high magnetic fields

Luc Van Bockstal and Fritz Herlach

Departement Natuurkunde, KU Leuven, Celestijnenlaan 200D, B-3030 Heverlee, Belgium

Received 2 April 1990

Abstract. The linewidth of the ferromagnetic resonance absorption in nickel, iron and cobalt was measured in pulsed magnetic fields up to 35 T at frequencies between 400 and 900 GHz. With this configuration we were able to determine the intrinsic relaxation in the temperature range between 10 and 300 K. Our results show that there is a universal behaviour of the relaxation for the 3d ferromagnets.

1. Introduction

For ferromagnetic resonances in metals at microwave frequencies, the position and the shape of the resonance absorption is well described by the Landau–Lifshitz–Gilbert equation [1,2] which describes the dynamics of the magnetisation $\boldsymbol{M}$:

$$\frac{\partial \boldsymbol{M}}{\partial t} = \gamma \boldsymbol{M} \times \left(\boldsymbol{B} + \frac{2A}{M_s^2} \nabla^2 \boldsymbol{M} - \frac{\lambda}{\gamma^2 M_s^2} \frac{4\pi}{\mu_0} \frac{\partial \boldsymbol{M}}{\partial t} \right) \tag{1}$$

where $\boldsymbol{B}$ is the magnetic field, A the molecular field exchange constant, and λ is a parameter for the intrinsic relaxation.

Solving equation (1) combined with Maxwell's equations and the appropriate boundary conditions gives a full description of the ferromagnetic resonance absorption in a metal. The solution shows that at low frequencies the linewidth of the resonance contains two contributions: the first is due to the intrinsic relaxation and is proportional to the λ parameter and to the frequency. Neglecting the exchange in the dynamics of the magnetisation would lead to a linewidth ΔB [3]

$$\gamma \Delta B = \frac{\lambda}{\gamma M_s} \frac{4\pi}{\mu_0} \omega. \tag{2}$$

The second contribution to the linewidth is called the exchange–conductivity broadening, and is due to the losses and the screening of the eddy currents. The broadening is proportional to the square root of frequency times conductivity [3]. At high frequencies it is not possible to find analytical expressions for the contributions of both mechanisms to the linewidth, but the dependencies are analogous to the low-frequency behaviour. As a result, the contribution of the intrinsic relaxation is more pronounced at high frequencies.

0953-8984/90/347187+07$03.50

At low temperatures the exchange–conductivity broadening is influenced by the out-of-phase behaviour of the electrical currents with respect to the electric field. At microwave frequencies the conductivity is altered by the non-local effects because the mean free path l of the electrons becomes larger than the penetration depth of the radiation. In the low-temperature limit, i.e. where the wavenumber k satisfies $|kl/(1 - i\omega\tau)| \ll 1$, the conductivity is given by [4]

$$\sigma_{T\to 0} = C_F/k \tag{3}$$

where $C_F = \frac{3}{4}\pi\sigma_{DC}/l$ is a constant depending on the Fermi surface of the metal.

The low-temperature behaviour of the conductivity at far infrared frequencies is different because the relaxation time τ of the electrons is much larger than the period of the radiation field. The condition for non-local conductivity, $|kl/(1 - i\omega\tau)| \ll 1$, is never reached and the conductivity is given by

$$\sigma = \sigma_{DC}\frac{1}{1 - i\omega\tau}. \tag{4}$$

At low temperatures, the velocity of the electrons is $\pi/2$ out of phase with the electric field and the real part of the conductivity is small. As a consequence, the dissipation and the line broadening due to the exchange–conductivity mechanism is small. This result shows that the resonances at far infrared frequencies are better suited for deducing the intrinsic relaxation from the linewidth of the resonances.

2. The experimental set-up

The resonance absorptions are measured in pulsed magnetic fields up to 35 T [5,6]. The magnetic fields are generated by discharging a 500 kJ capacitor bank into a resistive solenoid with 20 mm inner diameter. The pulse duration is of the order of 10 ms. The radiation between 400 and 900 GHz is provided by an optically pumped far-infrared (FIR) laser. The FIR radiation is guided by cylindrical waveguides through the cryostat and is detected by a n-InSb hot-electron detector in a separate He dewar. The sample is cooled by a flow of He gas, providing control of the temperature of the sample between 10 and 300 K.

Two sample configurations gave a satisfactory ferromagnetic resonance absorption: the metal powder suspension and the 'von Ortenberg' [7] strip line. With a first sample holder we measured the FIR transmission of a suspension of metal powder. The absorption is proportional to the real part of the surface impedance of the metal; the magnitude of the absorption can be controlled by the density of the powder. The broadening of the absorption profile due to inhomogeneous demagnetisation in the grains of the powder is a disadvantage of this method; this turned out to be negligible only in the case of the nickel powder. As a second configuration we used a strip line where the sample forms one wall of a narrow transmission line. With this method a well defined sample geometry is obtained and the absolute surface impedance of the metal can be calculated from the absorption coefficient of the strip line [7]. A disadvantage of this method is the loss in the coupling of the radiation to the strip line [8] resulting in a poor signal-to-noise ratio at the detector.

3. Results for nickel

The absorption of nickel was measured in the powder suspension and in the strip line. No broadening due to inhomogeneous demagnetisation was observed in the powder absorption. The relaxation parameter was determined by comparing the absorption with numerical simulations of the absorption for different values of λ using equation (1) and the conductivity as given by Chambers [4].

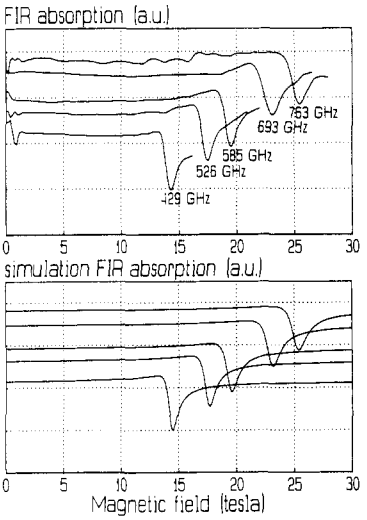

Figure 1. The absorption of nickel powder at 250 K for different FIR frequencies and numerical simulations of the absorption based on equation (1) and using $\lambda = 2.5 \times 10^8\ s^{-1}$.

Figure 1 shows the absorption of the nickel powder at 250 K for different FIR frequencies, together with the simulation of the absorption for the same frequencies using $\lambda = 2.5 \times 10^8\ s^{-1}$. A good agreement between the observed lineshape and the simulations is obtained, and the increase with frequency of the linewidth at high temperatures can be fitted with a constant λ parameter. Our results on the relaxation parameter λ and the data obtained at microwave frequencies [9, 10] show that the λ parameter is independent of frequency at temperatures above 120 K over a broad frequency range. Below 120 K the λ parameter increases and saturates at 60 K. The increase is independent of frequency at low frequencies [10] but is less pronounced at high frequencies (see figure 2).

The temperature and frequency dependencies can be explained assuming that the λ parameter contains two contributions. The first contribution is due to the non-resonant phonon scattering [11]:

$$\lambda_\rho = \chi_P (g-2)^2/\tau \tag{5}$$

where χ_P is the Pauli susceptibility, g the Landé factor and τ the relaxation time of the electron. Due to the factor $1/\tau$ this type of relaxation exhibits the same temperature dependence as the resistivity ρ.

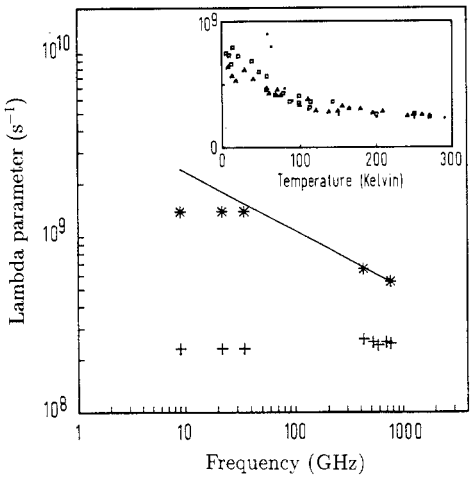

Figure 2. Relaxation parameter λ of nickel as a function of frequency at 250 K (*) and 25 K (+). The straight line shows an $\omega^{-1/3}$ dependence, as expected at high frequencies and low temperatures. The insert shows the temperature dependence of λ at 693 GHz (△), 429 GHz (□) and 22 GHz (•). The low-frequency data are taken from reference [10]

The other contribution is due to the deformation of the Fermi surface E_F by a magnetisation wave with amplitude m [12]:

$$\lambda_{\sigma+k} = \gamma^2 \left\langle n(\epsilon_F) \left| \frac{\partial E_F}{\partial (m/M_s)} \right|^2 \right\rangle \frac{\tan^{-1}(kl)}{kl} \tau. \tag{6}$$

where $n(\epsilon_F)$ is the density of states at the Fermi surface. This mechanism gives a temperature dependence similar to the non-local conductivity (see equation (3)): at high temperatures the λ parameter is proportional to the relaxation time τ—and thus to the conductivity—and at low temperatures λ is proportional to the inverse of the wavenumber k.

The high-temperature data on nickel shows that both relaxation mechanisms are equally strong around room temperature [13]; due to their opposite temperature dependence the total relaxation is constant over a broad temperature range.

At low temperatures the influence of the λ_ρ-type relaxation becomes small and the increase of λ is entirely due to the $\lambda_{\sigma+k}$ mechanism: at temperatures between 120 and 60 K the conductivity increases with decreasing temperature and hence so does the λ parameter; at temperatures below 60 K the conductivity and the wavenumber saturate (both at microwave and FIR frequencies).

To explain the differences in the low-temperature behaviour of λ as a function of frequency, two cases must be distinguished. At low frequencies, where the linewidth ΔB is smaller than the magnetisation $\mu_0 M_s$, there is an enhancement of the magnetic susceptibility at resonance (the Bloch–Bloembergen theory of resonance predicts $\chi'' = \mu_0 M_s / \Delta B$ at resonance). Taking into account this enhancement, which is related to the λ parameter by equation (2), and solving self-consistently for the wavenumber k from the non-local conductivity (equation (3)) and Maxwell's equations ($k^2 = i\omega\sigma\mu$), the λ parameter is independent of frequency at low temperatures. At high frequencies, where the linewidth is greater than the magnetisation, the magnetic permeability at

resonance does not differ much from the magnetic permeability of vacuum. When solving in the same way for the wavenumber k from the non-local conductivity and Maxwell's equations, k turns out to follow a $\omega^{1/3}$ rule. According to equation (6), the λ parameter is then proportional to $\omega^{-1/3}$. This dependence is shown as a straight line in figure 2. The crossover in the frequency behaviour occurs when the linewidth is equal to the magnetisation, which is in agreement with our results.

4. Results for iron

A comparison of the linewidth in the powder absorption and in the strip-line absorption showed that the broadening due to inhomogeneous demagnetisation in the powder was not negligible. Therefore only the data obtained with the strip line was analysed. The evolution of the relaxation parameter λ as a function of temperature was determined by comparing the linewidth of the absorption with the linewidth obtained by simulations for different values of λ for the whole temperature range.

Our first results [6] showed that the intrinsic relaxation gives only a small contribution to the linewidth of the resonance in iron. Because of this small contribution the data obtained at microwave frequencies do not permit an accurate determination of λ at low temperatures: in [14] the authors state that λ is almost constant at temperatures below 300 K, while the results in reference [15] indicate a sharp decrease of λ below 300 K.

After the development of a new strip line [8] we obtained data on the linewidth with sufficient accuracy to extract the contribution of the intrinsic damping. Figure 3 shows the evolution of the intrinsic damping parameter λ as a function of the temperature at 693 GHz. The full line is a fit based on the relaxation mechanisms in equations (5) and (6) using the values of λ_ρ and $\lambda_{\sigma+k}$ at room temperature as parameters (see also table 1). We used the value $C_F = 5 \times 10^{15}\ \Omega^{-1}\ m^{-2}$ for the anomalous conductivity, based on the value of C_F for chromium which has a Fermi surface similar to iron [16]. The increase of the relaxation below 120 K is due to the deformation of the Fermi surface. This behaviour was not observed at microwave frequencies because the contribution of the intrinsic damping to the linewidth is too small to be observed [14, 15].

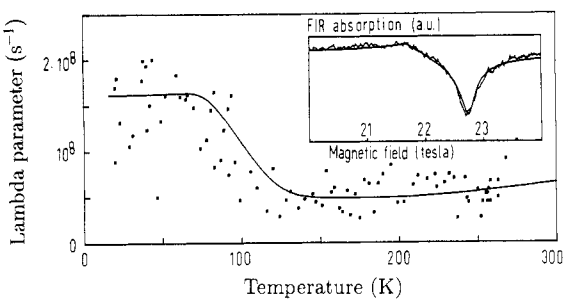

Figure 3. Relaxation parameter λ of iron at 693 GHz as a function of temperature. The insert shows the far infrared transmission of a strip line loaded with iron as a function of the magnetic field. The smooth curve is a simulation of the absorption using $\lambda = 0.7 \times 10^8\ s^{-1}$.

The insert in figure 3 shows the transmission of a strip line loaded with iron as a function of the magnetic field. The smooth curve is a simulation of the absorption using equation (1) and the conductivity as given by Chambers [4].

Table 1. Magnitude of the two damping mechanisms λ_ρ and $\lambda_{\sigma+k}$, which contribute to the λ parameter by the mechanisms given in equations (5) and (6), at room temperature determined from the evolution of λ as a function of the temperature. Also given are the magnetic and electrical parameters: the Landé factor, σ_{DC} and C_F.

	Nickel	Iron	Cobalt
$\lambda_\rho(273\ \mathrm{K})$ $(10^8\ \mathrm{s}^{-1})$	1.6	0.5	2.1
$\lambda_{\sigma+k}(273\ \mathrm{K})$ $(10^8\ \mathrm{s}^{-1})$	0.9	0.11	0.5
g	2.19	2.09	2.18
$\sigma_{DC}(273\mathrm{K})$ $(10^7\ \Omega^{-1}\ \mathrm{m}^{-1})$	1.28	1.00	1.02
C_F $(10^{15}\ \Omega^{-1}\ \mathrm{m}^{-2})$	3	5	16

5. Results for cobalt

The linewidth of the resonance absorption in cobalt was bigger than expected from the known values of the λ parameter. We attribute this to the large uniaxial anisotropy for the direction of the magnetisation, which causes the absorption to be inhomogeneously broadened in our polycrystalline samples. From the measurements of the magnetic anisotropy by means of ferromagnetic resonance at low temperatures in single-crystal samples [17], we estimate the line broadening to be 1.0 T.

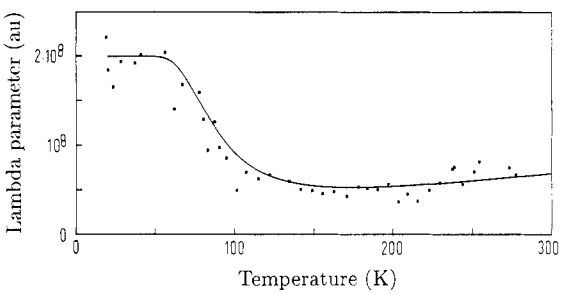

Figure 4. Relaxation parameter λ of cobalt at 763 GHz as a function of temperature.

After deduction of this contribution to the linewidth, we determined the relaxation parameter λ in the same way as for iron. The values obtained at 763 GHz are shown in figure 4. The full curve is a fit based on the relaxation mechanisms proposed in equations (5) and (6), using the parameters of table 1. The λ parameter is almost constant for temperatures between 120 and 300 K indicating that the two relaxation mechanisms (λ_ρ and $\lambda_{\sigma+k}$) are equally strong around 200 K. At temperatures below 120 K the relaxation increases and saturates around 60 K, showing the typical behaviour of the $\lambda_{\sigma+k}$-type relaxation.

6. Conclusion

Our results indicate that there is a universal behaviour of the intrinsic relaxation for the 3d metals: the relaxation is due to two mechanisms as given in equations (5) and (6). Around 250 K both mechanisms are equally strong and as they have an opposite

temperature dependence, the intrinsic relaxation is almost temperature independent between 120 and 300 K. At low temperatures the relaxation is dominated by the deformation of the Fermi surface (corresponding to the $\lambda_{\sigma+k}$-type relaxation). The increase below 120 K and the saturation around 60 K of the relaxation are explained by the temperature and frequency dependence of the mechanism proposed in equation (6).

As a general rule the strength of both relaxation mechanisms increases with increasing deviation of the g factor from the free electron value. This confirms the relations between the strength of both relaxation mechanisms and the spin–orbit coupling as worked out by Kambersky [11].

Acknowledgments

This work was supported by the Belgian Nationaal Fonds voor Wetenschappelijk Onderzoek and by the Onderzoeksraad of the KU Leuven.

References

[1] Gilbert T L 1955 *Phys. Rev.* 100 1243
[2] Landau L and Lifshitz E 1935 *Phyz. Z. Sowjet.* **8** 153
[3] Ament W S and Rado G T 1955 *Phys. Rev.* **97** 1558
[4] Chambers R G 1969 *The Physics of Metals, 1. Electrons* ed J M Ziman (Cambridge: Cambridge University Press)
[5] Herlach F, Van Bockstal L, van der Burgt M and Heremans G 1989 *Physica* B **155** 61
[6] Van Bockstal L, Dekoster J, Herlach F and Witters J 1989 *Physica* B **155** 332
[7] von Ortenberg M 1978 *Infrared Phys.* **18** 735
[8] Van Bockstal L, van der Burgt M and Herlach F 1989 *Digest 14th Int. Conf. on Infrared and Millimeter Waves, Würzburg, 1989* ed M von Ortenberg (Würzburg: SPIE, vol 1240) p 449
[9] Witters J, Herlach F and Van Bockstal L 1987 *Bull. Magn. Reson.* **8** 184
[10] Bhagat S M, Anderson J R and Hirst J J 1966 *Phys. Rev. Lett.* **16** 1099
[11] Kambersky V 1970 *Can. J. Phys.* **48** 2906
[12] Korenman V and Prange R E 1972 *Phys. Rev.* B **6** 2769
[13] Heinrich B, Meredith D J and Cochran J F 1979 *J. Appl. Phys.* **50** 7726
[14] Bhagat S M and Lubitz P 1974 *Phys. Rev.* B **1** 179
[15] Heinrich B and Frait Z 1966 *Phys. Status Solidi* **2** K11
[16] Chassaing G J and Sigrist M L 1973 *Thin Solid Films* **16** 37
[17] Frait Z and MacFadden H 1965 *Phys. Rev.* **139** A1173